ARTICLE

OBC
www.rsc.org/obc

Competing elimination and substitution reactions of simple acyclic disulfides†

Steven M. Bachrach* and Andrey Pereverzev‡
Department of Chemistry, Trinity University, 1 Trinity Place, San Antonio, TX, USA 78212.
E-mail: sbachrach@trinity.edu

Received 28th January 2005, Accepted 18th April 2005
First published as an Advance Article on the web 29th April 2005

MP2/aug-cc-pVDZ and B3LYP/cc-pVDZ calculations of the reactions of CH_3SSR (R = H or CH_3) with fluoride, hydroxide or allyl anion in the gas-phase were performed to determine the mechanism for both elimination and substitution reactions. The elimination reactions were shown to follow the E_2 mechanism. The substitution reactions with hydroxide and fluoride proceed by the addition–elimination mechanism, but those with allyl anion proceed by the S_N2 mechanism. The elimination reactions with F^- and HO^- are preferred to the substitution reactions, while allyl anion prefers the substitution route.

Introduction

Competition between substitution and elimination reactions provides an important example of the reactivity–selectivity relationships in the liquid phase.[1] The gas-phase anion–molecule counterpart is less well understood and some of the problems and steps taken to overcome them are related in a recent reviews by Gronert.[2,3] Gas-phase studies are hindered because the readily measured ionic product is identical for both mechanisms while the distinct neutral products are extremely difficult to detect.[4–6] This makes computer simulations an important tool in understanding the preferred mechanism whenever there is a competition between substitution and elimination pathways.

We have been interested in nucleophilic substitution at sulfur for some time. Nucleophilic attack at sulfur in sulfides,[7] acyclic disulfides,[8,9] and trisulfides[10] proceeds by an addition–elimination mechanism. The same is true for five- and six-membered cyclic disulfides, but small rings undergo substitution *via* the S_N2 mechanism.[11] We have noted evidence of the possibility of competing elimination reactions, especially in the reactions of methylsulfenyl derivatives with hydroxide and amide[7] and the reaction of dimethyldisulfide with thiolate.[8]

Grabowski and co-workers have examined the gas-phase reaction of dimethyl disulfide with a variety of nucleophiles.[12,13] The competition between substitution *vs.* elimination does not depend on the basicity of the nucleophile, but rather on its structure. Anions with localized charge preferentially induce an elimination reaction, while delocalized anions preferentially displace methylthiolate *via* a substitution pathway. In related work, Gronert, DePuy, and Bierbaum noted that for reactions of alkyl halides, the competition between substitution and elimination was also not controlled by the base strength of the nucleophile.[14,15]

Recently, the gas-phase reaction of alkylperoxides with fluoride has been examined both experimentally and computationally.[16] Elimination across the C–O bond is the dominant reaction. Computations suggest an E_2 mechanism, with a very small barrier.

In this paper we examine the reaction of two simple disulfides with fluoride, hydroxide, and allyl anion, comparing their substitution and elimination pathways (Scheme 1). The elimination proceeds by the E_2 path. The substitution reaction proceeds by an addition–elimination mechanism for F^- and HO^-, but is S_N2 for reaction with allyl anion. Elimination is kinetically favored over substitution for the reactions with F^- and HO^-, but substitution is favored for the reactions with allyl anion.

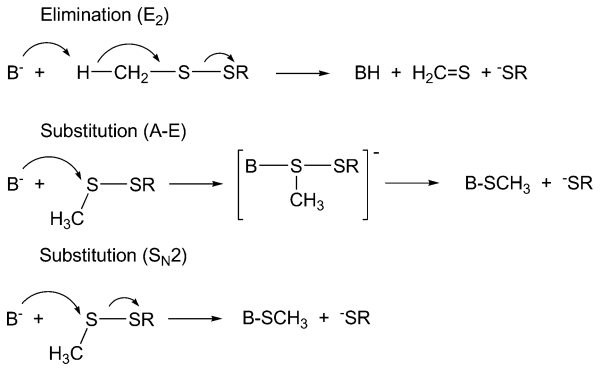

Scheme 1

Computational methods

Reactions (1)–(6) model elimination across the carbon–sulfur bond in disulfides. The first two reactions compare the effect of replacing hydrogen with methyl on the leaving group when the base is F^-. The same substituent effect is compared when the nucleophile is HO^- in reactions (3) and (4) and allyl anion in reactions (5) and (6). Reactions (7)–(12) model the competing nucleophilic substitution reactions at sulfur for the same reagents as in reactions (1)–(6).

Elimination reactions

$$F^- + CH_3SSH \rightarrow HF + H_2C{=}S + HS^- \quad (1)$$

$$F^- + CH_3SSCH_3 \rightarrow HF + H_2C{=}S + CH_3S^- \quad (2)$$

$$OH^- + CH_3SSH \rightarrow H_2O + H_2C{=}S + HS^- \quad (3)$$

$$OH^- + CH_3SSCH_3 \rightarrow H_2O + H_2C{=}S + CH_3S^- \quad (4)$$

$$CH_2{=}CHCH_2^- + CH_3SSH \rightarrow CH_2{=}CHCH_3 + H_2C{=}S + HS^- \quad (5)$$

$$CH_2{=}CHCH_2^- + CH_3SSCH_3 \rightarrow CH_2{=}CHCH_3 + H_2C{=}S + CH_3S^- \quad (6)$$

† Electronic supplementary information (ESI) available: Coordinates of all MP2/aug-cc-pVDZ and B3LYP/aug-cc-pVDZ optimized structures, their absolute energies, and number of imaginary frequencies. See http://www.rsc.org/suppdata/ob/b5/b501370d/

‡ Current address: Department of Chemistry, University of Houston, TX, USA

DOI: 10.1039/b501370d

Substitution reactions

$$F^- + CH_3SSH \rightarrow CH_3SF + HS^- \quad (7)$$

$$F^- + CH_3SSCH_3 \rightarrow CH_3SF + CH_3S^- \quad (8)$$

$$OH^- + CH_3SSH \rightarrow CH_3SOH + HS^- \quad (9)$$

$$OH^- + CH_3SSCH_3 \rightarrow CH_3SOH + CH_3S^- \quad (10)$$

$$CH_2{=}CHCH_2^- + CH_3SSH \rightarrow CH_3SCH_2CH_2{=}CH_2 + HS^- \quad (11)$$

$$CH_2{=}CHCH_2^- + CH_3SSCH_3 \rightarrow CH_3SCH_2CH_2{=}CH_2 + CH_3S^- \quad (12)$$

For all twelve reactions, the geometries of the reactants, products and transition states were fully optimized at MP2/aug-cc-pVDZ.[17,18] We have previously shown that this method performs well, in terms of geometry and energetic predictions, for substitution reactions at sulfur.[7–10] Analytic frequencies have been calculated for all species to obtain zero-point vibrational energies (ZPE) and to confirm the nature of the transition state. Analytical frequencies could not be performed for the critical points of reaction (6) and (12) due to insufficient scratch disk space. Because of this inability to confirm the nature of these critical points, and because of an interesting change in mechanism discussed below, we also optimized all of the structures (and computed their analytical frequencies) for reactions (5), (6), (11) and (12) using B3LYP/aug-cc-pVDZ.[19] This DFT method provides very similar geometries, relative energies, and topologies of the potential energy surfaces for nucleophilic substitution reactions at sulfur in simple, related systems.[9] In all cases, the zero-point energies were used without scaling. The frequencies were also used without scaling to determine 298 K thermal contributions to the free energies using standard partition-function approximations.[20] All computations were performed with GAUSSIAN-98[21] or GAUSSIAN-03.[22]

Results

Gas-phase E_2 reactions are characterized by having entrance and exit ion–dipole complexes (labeled **z-IDn** and **z-IDx**, respectively, where **z** is the reaction number) sandwiching a single transition state (labeled **z-TS**). A sketch of the potential energy surface (PES) for reaction (4), representative of a generic E_2 reaction, is shown in Fig. 1. All six elimination reactions have a topologically identical PES. Exit dipole complexes for reactions (5) and (6) were not located because of the size of the computations, but their existence is assumed.

The relative energies of all critical points for reactions (1)–(6) are listed in Table 1. Close examination of the electronic energies corrected for zero-point vibrational energy reveals that the transition state for reaction (2) lies below both ion–dipole complexes, and those for reactions (1), (3) and (4) lie below the entrance ion–dipole complexes. This is due to the ZPE corrections; these are true transition states on the electronic energy surface, as indicated by their having one imaginary frequency and energy above the ion–dipole complexes (as shown in parentheses in Table 1). While we have not optimized the geometry in terms of free energy, we do expect that there is a true transition state for all four reactions. What is clear is that the transition states will be very close in energy to the ion–dipole complexes.

Locating **5-IDn** and **6-IDn** was exceptionally difficult. The surface in the neighborhood is very flat with many local minima and transition states for interconversion among them. Optimization of the complex between allyl anion and CH_3SSCH_3 led to a structure where the allyl anion bridges between the two methyl groups, an ion–dipole complex that is unlikely to be on the reaction path for either substitution or elimination. **6-IDn** represents a structure where the allyl anion remains associated with only one of the methyl groups. The energies and geometries reported for **5-IDn** and **IDn** are likely not for the lowest energy ion–dipole complex, but rather just a representative example of the collection of possible ion–dipole structures.

The elimination reactions where the base is fluoride are endothermic, while those where the base is hydroxide or allyl anion

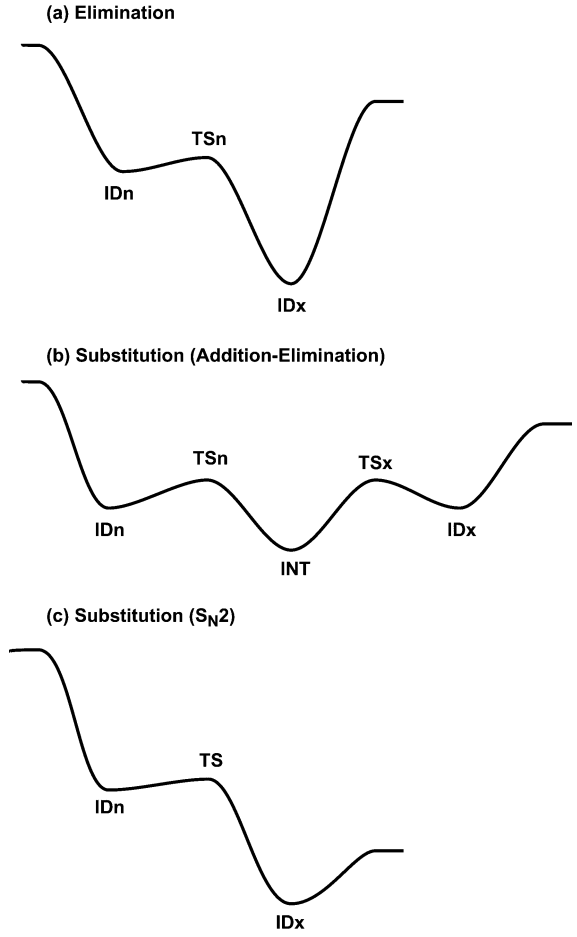

Fig. 1 Potential energy surfaces for the gas-phase (a) elimination reaction (reaction (4)), and substitution reactions by the (b) addition–elimination (reaction (8)) or (c) S_N2 (reaction (11)) mechanisms.

Table 1 Relative energies (kJ mol^{-1}) of the critical points for reactions (1)–(6)[a]

	Reactants	IDn	TS	IDx	Products
Reaction (1)	0.0	−82.8	−86.4	−90.6	1.0
	(0.0)	(−80.8)	(−71.4)	(−83.3)	(21.6)
	0.00	*−55.9*	*−57.8*	*−66.4*	*−37.6*
Reaction (2)	0.0	−79.2	−79.7	−76.8	50.2
	(0.0)	(−77.4)	(−65.3)	(−70.8)	(68.9)
	0.0	*−52.0*	*−51.0*	*−53.8*	*6.2*
Reaction (3)	0.0	−78.9	−84.5	−149.3	−79.2
	(0.0)	(−78.0)	(−77.2)	(−150.3)	(−67.8)
	0.0	*−50.0*	*−53.4*	*−125.9*	*−115.6*
Reaction (4)	0.0	−75.0	−81.2	−138.8	−30.2
	(0.0)	(−74.7)	(−73.1)	(−140.7)	(−20.5)
	0.0	*−46.0*	*−49.9*	*−114.7*	*−71.9*
Reaction (5)	0.0	−54.7	−71.3	—	−91.0
	(0.0)	(−57.5)	(−66.7)	—	(−78.2)
	0.0	*−13.9*	*−27.4*	—	*−116.0*
Reaction (6)	(0.0)	(−56.0)	(−44.8)	—	(−30.9)

[a] The top values are relative electronic energies corrected for zero-point vibrational energies all evaluated at MP2/aug-cc-pVDZ. The middle values, in parentheses, are the relative electronic energies alone. The bottom values, in italics, are the relative Gibbs free energies.

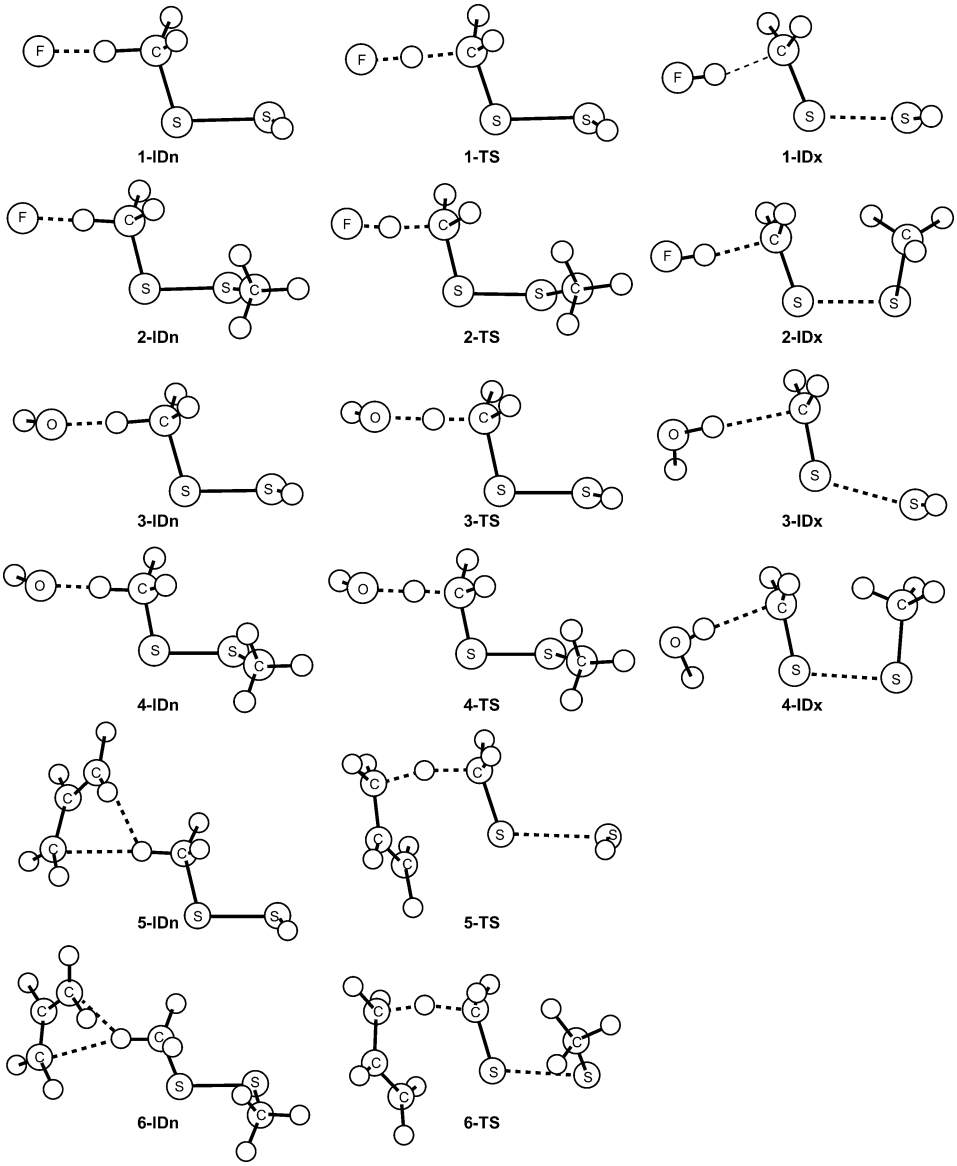

Fig. 2 Drawings of the MP2/aug-cc-pVDZ optimized structures for reactions (1)–(6).

are exothermic. This reflects the fact that hydroxide ($PA(HO^-)$ = 1633 kJ mol^{-1}) and allyl anion ($PA(CH_2{=}CHCH_2^-)$ = 1628 kJ mol^{-1}) are stronger bases than fluoride ($PA(F^-)$ = 1554 kJ mol^{-1}).[23] The reactions of dimethyldisulfide (reactions (2), (4) and (6)) are less exothermic than the reactions of methyldisulfide (reactions (1), (3) and (5)). This is also a reflection of base strength: methylthiolate is a stronger base ($PA(CH_3S^-)$ = 1496 kJ mol^{-1}), and therefore a poorer leaving group, than thiolate ($PA(HS^-)$ = 1468 kJ mol^{-1}).[23] When Gibbs free energies are examined, reactions (1), (3), (4) and (5) are exoergonic (reaction (6) is likely exoergonic, see below), while reaction (2) is slightly endoergonic.

The optimized geometries of all critical points for reactions (1)–(6) are drawn in Fig. 2. Important distances in these structures are listed in Table 2. The bond changes occur in a concerted fashion all the way through the reaction path. So, in every step as one proceeds from reactants, to **IDn**, to **TS**, to **IDx** and finally to products, the S–S bond lengthens, the C–S bond shortens, the C–H bond lengthens, and the X–H bond shortens (where X = F for reactions (1) and (2), and X = O for reactions (3) and (4) and X = C for reaction (5) and (6)).

The transition state reflects these concerted bond changes, in the appropriate lengthening/shrinking of distances. Further, atomic motion in the imaginary frequency for each transition state shows concerted (i) H–F, H–O or H–C bond formation, (ii) C–S bond contraction, and (iii) S–S bond rupture. The breaking C–H bond is antiperiplanar to the cleaving S–S bond – the H–C–S–S dihedral angle ranges from 177.5° to 181.1° in the transition states. This behavior is indicative of a synchronous E_2 reaction mechanism.

The transition states involving hydroxide, **3-TS** and **4-TS**, are noticeably earlier than the transition states involving fluoride, **1-TS** and **2-TS**. The C–H distances are about 0.15 Å shorter, the C–S distances are 0.03 Å longer and the S–S distances are about 0.05 Å shorter in the hydroxide TSs than in the fluoride TSs. This is completely consistent with the Hammond Postulate: the hydroxide reactions are much more exothermic than the fluoride cases and so should have much earlier transition states. This argument would suggest that the structures of **5-TS** and **6-TS** should be similar to **3-TS** and**4-TS** since they have comparable energetics. However, the TSs for the reactions with allyl anion are later than the other four TSs; note that the C–S distance is shorter and the S–S distance is longer in **5-TS** and **6-TS** than in the others. Unlike in reactions (1)–(4), the allyl anion can remove the proton with one terminal carbanion while simultaneously providing some nucleophilic assistance at sulfur with the other terminal carbanionic center. This nucleophilic assistance serves to promote the cleavage of the S–S bond.

In their experimental study of the gas-phase reaction between dimethyldisulfide and various anions, Grabowski and Zhang[12]

Table 2 Important distances (Å) in the optimized structures for reactions (1)–(6)

	F–H	C–H	C–S	S–S
Reaction (1)				
Reactants	—	1.099	1.827	2.093
1-IDn	1.550	1.163	1.810	2.117
1-TS	1.164	1.400	1.753	2.192
1-IDx	0.968	1.868	1.681	2.481
Products	0.925	—	1.631	—
Reaction (2)				
Reactants	—	1.099	1.829	2.084
2-IDn	1.557	1.161	1.815	2.103
2-TS	1.121	1.454	1.754	2.180
2-IDx	0.967	1.874	1.685	2.479
Products	0.925	—	1.631	—
	O–H	**C–H**	**C–S**	**S–S**
Reaction (3)				
Reactants	—	1.099	1.827	2.093
3-IDn	1.617	1.172	1.807	2.121
3-TS	1.441	1.248	1.788	2.142
3-IDx	0.980	2.227	1.674	2.579
Products	0.966	—	1.631	—
Reaction (4)				
Reactants	—	1.099	1.829	2.084
4-IDn	1.633	1.166	1.813	2.105
4-TS	1.409	1.266	1.791	2.128
4-IDx	0.979	2.258	1.683	2.616
Products	0.966	—	1.631	—
	C–H	**C–H**	**C–S**	**S–S**
Reaction (5)				
Reactants	—	1.099	1.827	2.093
5-IDn	2.324	1.109	1.827	2.105
5-TS	1.336	1.416	1.725	2.744
Products	1.102	—	1.631	—
Reaction (6)				
Reactants	—	1.099	1.829	2.084
6-IDn	2.341	1.108	1.828	2.095
6-TS	1.378	1.373	1.733	2.654
Products	1.102	—	1.631	—

identified the $CH_3SCH_2S^-$ anion as the ultimate product of the elimination reaction. This anion results from a nucleophilic addition of the products of the elimination reaction, $H_2C{=}S$ and CH_3S^-. We have also calculated the energetics of the analogous reactions (reaction (13)), which are listed in Table 3. The ion dipole complex, transition state and products for these two reactions are drawn in Fig. 3. The addition of either thiolate or methylthiolate to thioformaldehyde is a very exoergonic reaction, −70.9 and −104.9 kJ mol^{-1}, respectively. The barriers are very small, lying below separated reactants and only 4–8 kJ mol^{-1} above the ion dipole complex.

Table 3 Relative energies (kJ mol^{-1}) for reactions (13a) and (13b)[a]

Reaction	Reactants	Ion–dipole	**TS**	Product
(13a)	0.0	−44.3	−43.3	−103.8
	0.0	*−22.0*	*−15.9*	*−70.9*
(13b)	0.0	−48.7	−46.5	−144.9
	0.0	*−21.0*	*−17.6*	*−104.9*

[a] The top values are relative electronic energies corrected for zero-point vibrational energies all evaluated at MP2/aug-cc-pVDZ. The bottom values, in italics, are the relative Gibbs free energies.

$$HS^- + H_2C{=}S \rightarrow HSCH_2S^- \quad (13a)$$

$$CH_3S^- + H_2C{=}S \rightarrow CH_3SCH_2S^- \quad (13b)$$

Our previous studies of nucleophilic substitution at sulfur determined that the reaction mechanism is addition–elimination (A–E).[7–11,24] We find that reactions (7)–(10) are no exception; each reaction surface is characterized by entrance and exit ion–dipole complexes, and entrance (**z-TSn**) and exit (**z-TSx**) transition states surrounding a stable intermediate (**z-INT**). The triple-well potential energy surface for reaction (8), representative of a generic A–E mechanism, is shown in Fig. 1. All four substitution reactions (7)–(10) have topologically identical PESs.

The relative energies of all critical points for reactions (7)–(10) are listed in Table 4 and their structures are shown in Fig. 4. We assume that the entrance ion–dipole complexes for the elimination and substitution reactions will be identical. Nucleophilic substitution at sulfur by fluoride is endothermic, while attack by hydroxide is exothermic.

In these four reactions, the intermediate is the lowest point on the reaction surface. The depth of this intermediate well is the characteristic feature of the addition–elimination reaction. The intermediates for nucleophilic substitution at sulfur typically lie in wells about 8–20 kJ mol^{-1} deep.[7–11,24] For reactions (7) and (8), the reverse barriers for the first step fall in the normal range: 16.4 and 7.0 kJ mol^{-1}, respectively. However, the forward barriers for the second step are very large: 62.5 kJ mol^{-1} for reaction (7) and 88.0 kJ mol^{-1} for reaction (8). The opposite is the case for reaction (9); here, the forward barrier for the second step is normal (12.1 kJ mol^{-1}) and the reverse barrier of the first step is large (49.1 kJ mol^{-1}). The intermediate for reaction (10) lies in a more symmetric well, with both barriers about 30 kJ mol^{-1}. The shapes of these wells are in part a reflection of the overall reaction energetics. The reactions with fluoride are endothermic, while the reactions of hydroxide are exothermic. The barrier heights from the intermediate reflect whether the products or reactants are energetically more favorable; the lower

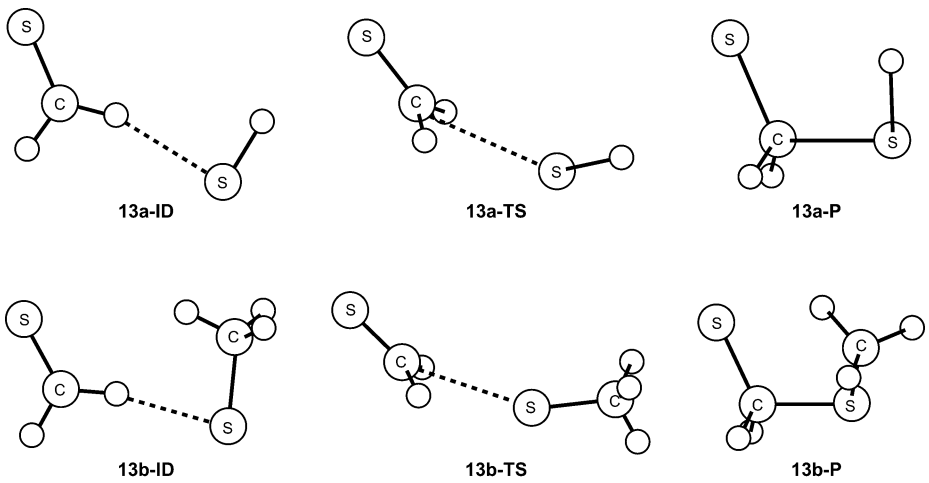

Fig. 3 Drawings of the MP2/aug-cc-pVDZ optimized structures for reaction (13).

Table 4 Relative energies (kJ mol^{-1}) of the critical points for reactions (7)–(12)[a]

Reaction	Reactants	IDn	TSn	INT	TSx	IDx	Products
(7)	0.0	−82.8	−76.8	−93.2	−30.7	−31.7	24.8
	(0.0)	(−80.8)	(−76.2)	(−93.7)	(−26.3)	(−27.9)	(30.0)
	0.0	*−55.9*	*−46.0*	*−63.8*	*−8.7*	*−12.3*	*18.6*
(8)	0.0	−79.2	−71.6	−78.6	9.4	3.8	73.9
	(0.0)	(−77.4)	(−71.2)	(−79.3)	(11.2)	(6.1)	(77.4)
	0.0	*−52.0*	*−40.6*	*−50.0*	*36.4*	*28.6*	*62.4*
(9)	0.0	−78.9	−75.7	−124.8	−112.6	−113.1	−72.0
	(0.0)	(−78.3)	(−76.8)	(−130.8)	(−117.6)	(−118.2)	(−75.6)
	0.0	*−50.0*	*−43.4*	*−92.5*	*−83.2*	*−89.5*	*−73.0*
(10)	0.0	−75.0	−71.0	−100.5	−70.7	−74.2	−22.8
	(0.0)	(−74.7)	(−72.8)	(−107.3)	(−78.2)	(−81.1)	(−28.3)
	0.0	*−46.0*	*−38.4*	*−68.1*	*−40.2*	*−47.5*	*−29.3*
(11)	0.0	−54.7	−60.4	—	—	−212.9	−184.1
	(0.0)	(−57.5)	(−63.6)	—	—	(−223.8)	(−194.1)
	0.0	*−13.9*	*−17.9*	—	—	*−181.3*	*−175.8*
(12)	(0.0)	(−56.0)	(−58.9)	—	—	(−184.3)	(−146.8)

[a] The top values are relative electronic energies corrected for zero-point vibrational energies all evaluated at MP2/aug-cc-pVDZ. The middle values, in parentheses, are the relative electronic energies alone. The bottom values, in italics, are the relative Gibbs free energies.

barrier pairs with the less energetic of the reactant or product. This is a manifestation of the Hammond Postulate.

The values of some geometric parameters along the pathway for reactions (7)–(10) are given in Table 5. As one would expect, the X–S bond is smoothly made and the S–S bond is smoothly cleaved as these reactions progress from reactant to intermediate to product. The S–S distance in **9-INT** and **10-INT** are similar to values in intermediates of other substitution reactions of di- and trisulfides.[8–10] However, the S–S bond is much shorter in **7-INT** and **8-INT**. Further support for classification of the mechanism is apparent in the geometries of the transition states and intermediates. An S_N2 transition state is expected to have a near-linear arrangement of nucleophile, atom under attack and leaving group. This arrangement, does in fact occur, but in the *intermediates* of reactions (7)–(10). In all of the transition states, this angle is about 150–160°.

The PES for nucleophilic substitution by allyl anion is decidedly different. We were able to locate only one transition state and no intermediates, despite extensive searching for them, for reactions (11) and (12) using MP2/aug-cc-pVDZ. We were able to characterize these structures by computing analytical frequencies for reaction (11), but the disk space required for these calculations for reaction (12) exceeded our resources. The relative energies are given in Table 4 and the structures are drawn in Fig. 4. Since the MP2 results are suggestive of a different mechanism for reaction with allyl anion than with any of the other nucleophiles we have examined, we repeated the optimization using B3LYP/aug-cc-pVDZ to allay any concern that these results might be simply a manifestation of a poor computational method. We had previously demonstrated that B3LYP, MP2, and CISD all predict the addition–elimination mechanism for the thiolate–disulfide exchange.[8,9]

The B3LYP relative energies for the critical points along reactions (5), (6), (11) and (12) are listed in Table 6. All structures were confirmed to be local minima or transition states by evaluation of the analytical Hessian matrix. The geometries of these structures vary little from the MP2 structures, with full details given in the Supporting information.†

For reactions (5) and (6), a single transition state was located, indicative of the E_2 mechanism. The overall reaction energetics are similar for the two computational methods, but the B3LYP transition states are predicted to be higher in energy with B3LYP than MP2.

The B3LYP results for reactions (11) and (12) are also similar to those obtained at MP2. No intermediate was located. A single TS is found for each reaction. Again they are higher in energy at B3LYP than at MP2. B3LYP predicts both reactions are less exothermic than with MP2. Since the two methods, which treat electron correlation in very different ways, give the same topology for the PES of reactions (11) and (12), and the

Table 5 Important distances (Å) and angles (°) in the optimized structures for reactions (7)–(12)

	F–S	S–S	F–S–S
Reaction (7)			
Reactants	—	2.093	—
7-IDn	3.645	2.117	150.2
7-TSn	2.912	2.127	166.9
7-INT	2.029	2.324	177.6
7-TSx	1.711	4.223	155.7
7-IDx	1.713	4.279	153.3
Products	1.685	—	—
Reaction (8)			
Reactant	—	2.084	—
8-IDn	3.680	2.103	148.7
8-TSn	2.837	2.115	168.2
8-INT	2.123	2.244	176.9
8-TSx	1.715	4.154	153.7
8-IDx	1.729	4.205	150.8
Products	1.685	—	—
	O–S	**S–S**	**O–S–S**
Reaction (9)			
Reactant	—	2.093	—
9-IDn	3.707	2.121	151.1
9-TSn	3.290	2.122	160.6
9-INT	1.925	2.587	178.4
9-TSx	1.751	3.971	163.6
9-IDx	1.746	4.451	151.6
Products	1.721	—	—
Reaction (10)			
Reactant	—	2.084	—
10-IDn	3.758	2.105	149.1
10-TSn	3.219	2.108	161.4
10-INT	1.998	2.457	178.0
10-TSx	1.749	4.012	159.6
10-IDx	1.751	4.360	150.7
Products	1.721	—	—
	C–S	**S–S**	**C–S–S**
Reaction (11)			
Reactant	—	—	—
11-IDn	4.994	2.105	122.8
11-TS	3.394	2.143	170.0
11-IDx	1.841	4.784	140.7
Products	1.841	—	—
Reaction (12)			
Reactant	—	—	—
12-IDn	4.966	2.094	121.9
12-TS	3.509	2.116	169.6
12-IDx	1.822	4.550	142.5
Products	1.841	—	—

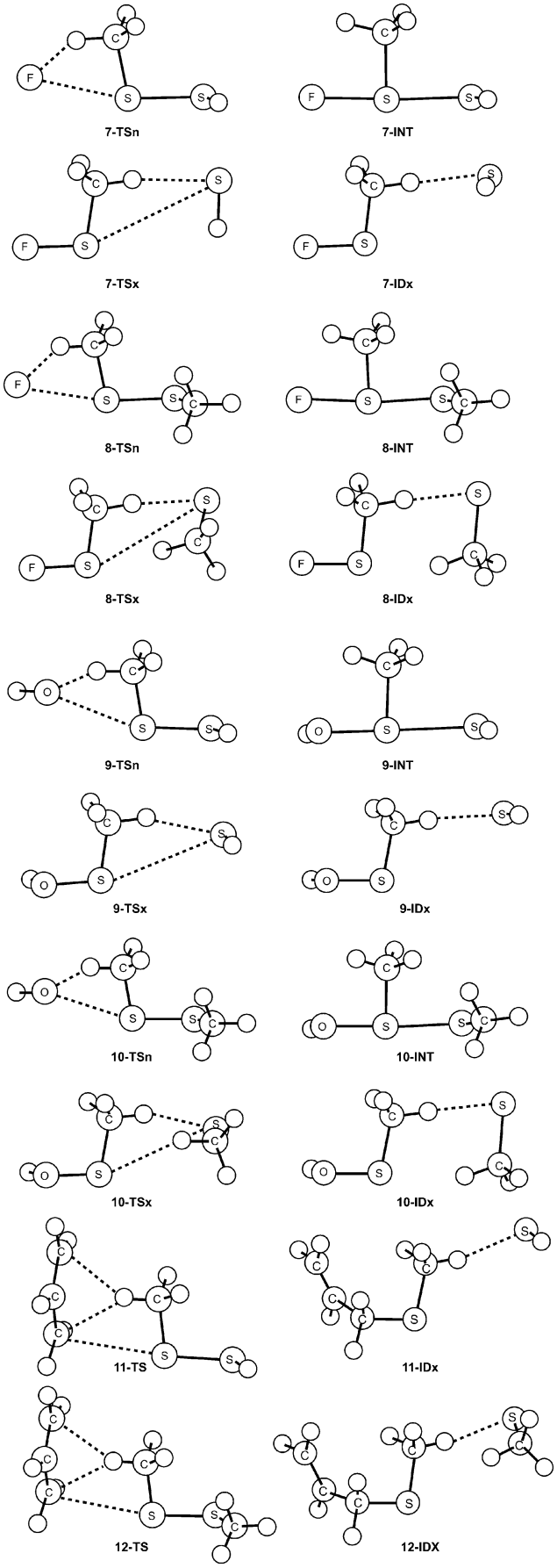

Fig. 4 Drawings of the MP2/aug-cc-pVDZ optimized structures for reactions (7)–(12).

two methods give very similar geometries for **TS-11** and **TS-12**, we conclude that these two reactions proceed *via* a different mechanism than reactions (7)–(10).

Table 6 B3LYP relative energies (kJ mol^{-1}) of the critical points for reactions (5), (6), (11) and (12)[a]

Reaction	Reactants	**IDn**	**TS**	**IDx**	Products
(5)	0.0	−41.4	−38.7	—	−75.0
	(0.0)	(−43.0)	(−32.3)	—	(−72.7)
	0.0	*−9.0*	*2.5*	—	*−109.8*
(6)	0.0	−30.8	−23.8	—	−32.6
	(0.0)	(−34.8)	(−16.1	—	(−31.4)
	0.0	*11.2*	*11.6*	—	*−74.5*
(11)	0.0	−41.4	−52.1	−175.7	−154.0
	(0.0)	(−43.0)	(−55.4)	(−186.9)	(−164.0)
	0.0	*−9.0*	*−10.7*	*−142.5*	*−146.0*
(12)	0.0	−30.8	−42.1	−134.9	−111.5
	(0.0)	(−34.8)	(−44.9)	(−147.0)	(−122.7)
	0.0	*11.2*	*−3.3*	*−105.1*	*−110.6*

[a] The top values are relative electronic energies corrected for zero-point vibrational energies all evaluated at B3LYP/aug-cc-pVDZ. The middle values, in parentheses, are the relative electronic energies alone. The bottom values, in italics, are the relative Gibbs free energies.

The gas-phase S_N2 surface is characterized by entrance and exit ion–dipole complexes separated by a single transition state,[25] consistent with the results for reactions (11) and (12). The PES for reaction (11) is shown in Fig. 1. The geometry of an S_N2 transition state is characterized by the backside attack of the nucleophile, leading to a near-linear arrangement of nucleophile, substrate and leaving group. The corresponding angle ($C^-\cdot S\cdot S$) in **TS-11** is 170.0° (MP2) or 172.2° (B3LYP), and 169.6° (MP2) or 172.1° (B3LYP) in **TS-12**. Therefore, these two reactions proceed by the S_N2 mechanism.

The reasons for the change of mechanism from what we have typically found for reactions at sulfur (addition–elimination) with allyl anion are under current investigation. What concerns us in this work is the competition between substitution and elimination. B3LYP predicts that substitution is both kinetically and thermodynamically favored over elimination for both reactions with allyl anion. The MP2 results are in concurrence, except that **TS-5** is lower in enthalpy (and free energy) than **TS-11**, indicating elimination is kinetically preferred in this case.

Discussion

Elimination across the C–S bond in disulfides has been studied here using fluoride, hydroxide or allyl anion as the base. The reactions with F^- are not favorable when considering just the electronic energy. However, with the additional consideration of entropy, reaction (1) is exoergonic and reaction (2) is essentially thermoneutral. This is in contrast to the elimination reaction of F^- with CH_3OOH, which is predicted to have a reaction energy of −149.8 kJ mol^{-1}.[16] This difference is due to the differential bond energies that are made and broken; the peroxide reaction is favored over the disulfide because of the O–O bond that is broken is weaker than the S–S bond and the C=O bond that is formed is stronger than the C=S bond. The elimination reactions where hydroxide or allyl anion is the base are exoergonic. These reactions are driven by hydroxide and allyl anion being stronger bases than fluoride.

All six elimination reactions proceed by the E_2 mechanism. Each reaction has a single transition state where motion to break the C–H and S–S bonds and form the C–S double bond are all taking place in a concerted fashion. The two cleaving bonds are in an antiperiplanar arrangement. There are no intermediates (other than the ion–dipole complexes) along the reaction pathway. The TSs for the reactions with allyl anion indicate a cooperative nucleophilic assistance by the other terminal carbanion in displacing the leaving group in this elimination step.

Grabowski and Zhang[12] observed predominantly elimination products for the reaction of hydroxide with dimethyldisulfide.

They proposed that the product observed was actually $CH_3SCH_2S^-$, formed by the addition of the true elimination products CH_3S^- and $H_2C{=}S$. Our calculations indicate that this addition is favorable with a very small activation barrier.

Furthermore, our calculations indicate that elimination should dominate substitution for reactions (1)–(4). For these four cases, the elimination pathway is more exoergonic than the substitution pathway. The preference is not simply entropic, which would favor elimination (which creates three molecules from two) over substitution (where there is no net change in the number of molecules). The elimination reactions are more exothermic than their substitution partners, by about 25 kJ mol^{-1} for the reactions with F^- and about 8 kJ mol^{-1} for the reactions with HO^-.

More importantly, kinetics favors elimination over substitution for these localized bases, and the gas-phase experiments are likely to be under kinetic control. For the two fluoride reactions, the transition state for the elimination reaction is lower in energy than the *lower* of the two substitution transition states, let alone the rate-limiting *higher*-lying transition state. For the hydroxide reactions, the elimination transition states (**3-TS** and **4-TS**) are about 8 kJ mol^{-1} lower in energy than the higher transition states of the substitution path (**9-TSn** and **10-TSn**).

In contrast, Grabowski and Zhang[12] observed predominantly substitution products for the reaction of allyl anion with dimethyldisulfide. Our computations also indicate a preference for substitution over elimination. The substitution reactions (reactions (11) and (12)) are much more exothermic and exoergonic than their elimination counterparts (reaction 5 and 6). However, it is the kinetic preference that bears upon comparison with experiment. For the reaction of allyl anion with dimethyldisulfide, substitution is kinetically favored over elimination. The kinetic situation is less clear for the reaction of allyl anion with methyldisulfide. MP2 suggests that **TS-5** is lower in enthalpy than **TS-11**, though this difference is less than 10 kJ mol^{-1}. B3LYP predicts the opposite order, with **TS-11** 14 kJ mol^{-1} lower in enthalpy than **TS-5**. Thus, B3LYP is consistent in indicating that substitution is kinetically favored for both reactions involving allyl anion.

Grabowski and Zhang[12] speculated that the different reaction preferences were due to the localized *versus* delocalized nature of the nucleophile/base. Our computations are in agreement with this observation. Further, allyl anion appears to follow an S_N2 pathway rather than the addition–elimination pathway we have observed for a large range of charge-localized nucleophiles.[7–11] We are currently examining a series of charge-delocalized nucleophiles to assess the underlying cause of this behavior. These results will be published in due course.

Conclusions

These computations are in complete agreement with the experimental findings.[12] The localized hard bases examined here, F^- and HO^-, will preferentially induce an elimination reaction with disulfides, rather than the substitution alternative. Elimination is favored both kinetically and thermodynamically. The elimination reaction follows an E_2 mechanism, while the substitution path occurs *via* an addition–elimination mechanism. On the other hand, the delocalized soft base allyl anion prefers to follow a substitution pathway over elimination in its reactions with disulfides, and the mechanism for this substitution reaction is S_N2.

Acknowledgements

We are grateful to the National Science Foundation (CHE-0307260) and the Robert A. Welch Foundation (W-1442) for support of this research. We thank the two anonymous reviewers for many helpful suggestions.

References

1 M. B. Smith and J. March, *March's Advanced Organic Chemistry: Reactions, Mechanisms, and Structure*, Wiley, New York, 2001.
2 S. Gronert, *Chem. Rev.*, 2001, **101**, 329.
3 S. Gronert, *Acc. Chem. Res.*, 2003, **36**, 848.
4 C. A. Lieder and J. I. Brauman, *Int. J. Mass Spectrom. Ion Phys.*, 1975, **16**, 307.
5 M. E. Jones and G. B. Ellison, *J. Am. Chem. Soc.*, 1989, **111**, 1645.
6 R. C. Lum and J. J. Grabowski, *J. Am. Chem. Soc.*, 1988, **110**, 8568.
7 S. M. Bachrach and B. D. Gailbreath, *J. Org. Chem.*, 2001, **66**, 2005.
8 S. M. Bachrach and D. C. Mulhearn, *J. Phys. Chem.*, 1996, **100**, 3535.
9 S. M. Bachrach, J. M. Hayes, T. Dao and J. L. Mynar, *Theor. Chem. Acc.*, 2002, **107**, 266.
10 D. C. Mulhearn and S. M. Bachrach, *J. Am. Chem. Soc.*, 1996, **118**, 9415.
11 S. M. Bachrach, J. T. Woody and D. C. Mulhearn, *J. Org. Chem.*, 2002, **67**, 8983.
12 J. J. Grabowski and L. Zhang, *J. Am. Chem. Soc.*, 1989, **111**, 1193.
13 J. K. Lee and J. J. Grabowski, *J. Org. Chem.*, 1996, **61**, 9422.
14 S. Gronert, C. H. DePuy and V. M. Bierbaum, *J. Am. Chem. Soc.*, 1991, **113**, 4009.
15 S. Gronert, *J. Am. Chem. Soc.*, 1991, **113**, 6041.
16 S. J. Blanksby, G. B. Ellison, V. M. Bierbaum and S. Kato, *J. Am. Chem. Soc.*, 2002, **124**, 3196.
17 T. H. J. Dunning, *J. Chem. Phys.*, 1989, **90**, 1007.
18 D. Woon and T. H. J. Dunning, *J. Chem. Phys.*, 1993, **98**, 1358.
19 (*a*) A. D. Becke, *J. Chem. Phys.*, 1993, **98**, 5648; (*b*) C. Lee, W. Yang and R. G. Parr, *Phys. Rev. B: Condens. Matter*, 1988, **37**, 785; (*c*) S. H. Vosko, L. Wilk and M. Nusair, *Can. J. Phys.*, 1980, **58**, 1200; (*d*) P. J. Stephens, F. J. Devlin, C. F. Chabalowski and M. J. Frisch, *J. Phys. Chem.*, 1998, **98**, 11623.
20 C. J. Cramer, *Essentials of Computational Chemistry. Theories and Models*, John Wiley, Chichester, UK, 2002.
21 M. J. Frisch, G. W. Trucks, H. B. Schlegel, G. E. Scuseria, M. A. Robb, J. R. Cheeseman, V. G. Zakrzewski, J. A. Montgomery, Jr., R. E. Stratmann, J. C. Burant, S. Dapprich, J. M. Millam, A. D. Daniels, K. N. Kudin, M. C. Strain, O. Farkas, J. Tomasi, V. Barone, M. Cossi, R. Cammi, B. Mennucci, C. Pomelli, C. Adamo, S. Clifford, J. Ochterski, G. A. Petersson, P. Y. Ayala, Q. Cui, K. Morokuma, D. K. Malick, A. D. Rabuck, K. Raghavachari, J. B. Foresman, J. Cioslowski, J. V. Ortiz, A. G. Baboul, B. B. Stefanov, G. Liu, A. Liashenko, P. Piskorz, I. Komaromi, R. Gomperts, R. L. Martin, D. J. Fox, T. Keith, M. A. Al-Laham, C. Y. Peng, A. Nanayakkara, C. Gonzalez, M. Challacombe, P. M. W. Gill, B. G. Johnson, W. Chen, M. W. Wong, J. L. Andres, M. Head-Gordon, E. S. Replogle and J. A. Pople, *GAUSSIAN 98 (Revision A.7)*, Gaussian, Inc., Pittsburgh, PA, 1998.
22 M. J. Frisch, G. W. Trucks, H. B. Schlegel, G. E. Scuseria, M. A. Robb, J. R. Cheeseman, J. A. Montgomery, Jr., T. Vreven, K. N. Kudin, J. C. Burant, J. M. Millam, S. S. Iyengar, J. Tomasi, V. Barone, B. Mennucci, M. Cossi, G. Scalmani, N. Rega, G. A. Petersson, H. Nakatsuji, M. Hada, M. Ehara, K. Toyota, R. Fukuda, J. Hasegawa, M. Ishida, T. Nakajima, Y. Honda, O. Kitao, H. Nakai, M. Klene, X. Li, J. E. Knox, H. P. Hratchian, J. B. Cross, V. Bakken, C. Adamo, J. Jaramillo, R. Gomperts, R. E. Stratmann, O. Yazyev, A. J. Austin, R. Cammi, C. Pomelli, J. Ochterski, P. Y. Ayala, K. Morokuma, G. A. Voth, P. Salvador, J. J. Dannenberg, V. G. Zakrzewski, S. Dapprich, A. D. Daniels, M. C. Strain, O. Farkas, D. K. Malick, A. D. Rabuck, K. Raghavachari, J. B. Foresman, J. V. Ortiz, Q. Cui, A. G. Baboul, S. Clifford, J. Cioslowski, B. B. Stefanov, G. Liu, A. Liashenko, P. Piskorz, I. Komaromi, R. L. Martin, D. J. Fox, T. Keith, M. A. Al-Laham, C. Y. Peng, A. Nanayakkara, M. Challacombe, P. M. W. Gill, B. G. Johnson, W. Chen, M. W. Wong, C. Gonzalez and J. A. Pople, *GAUSSIAN 03 (Revision C.02)*, Gaussian, Inc., Wallingford, CT, 2004.
23 W. G. Mallard and P. J. Linstrom, in *NIST Chemistry Webbook – March 2003 Release*, NIST, Gaithersburg, MD, 2003.
24 J. M. Hayes and S. M. Bachrach, *J. Phys. Chem A*, 2003, **107**, 7952.
25 W. N. Olmstead and J. I. Brauman, *J. Am. Chem. Soc.*, 1977, **99**, 4219.